Antiangiogenesis Targeting Tumor Microenvironment Synergizes Glucuronide Prodrug Antitumor Activity

Ting-Yi Juan,[1,4,6] Steve R. Roffler,[6] Hsien-San Hou,[4,6] Shih-Ming Huang,[4,5] Kai-Chuan Chen,[6,7] Yu-Lin Leu,[8] Zeljko M. Prijovich,[6] Cheng-Ping Yu,[3,4] Chang-Chieh Wu,[2] Guang-Huan Sun,[1,4] and Tai-Lung Cha[1,4]

Abstract

Purpose: This study is aimed at investigating the *in vivo* antitumor activity of a novel cell-impermeable glucuronide prodrug, 9-aminocamptothecin glucuronide (9ACG), and elucidating the synergistically antitumor effects of antiangiogenesis therapy by targeting the tumor microenvironment.

Experimental Design: We analyzed the antitumor effects of 9ACG alone or combined with anti-angiogenic monoclonal antibody DC101 on human tumor xenografts by measuring tumor growth and mouse survival in BALB/c *nu*/*nu* nude and NOD/SCID mice. The drug delivery, immune response, and angiogenesis status in treated tumors were assessed by high performance liquid chromatography, immunohistochemistry, and immunofluorescence assays.

Results: We developed a nontoxic and cell-impermeable glucuronide prodrug, 9ACG, which can only be activated by extracellular β-glucuronidase to become severely toxic. 9ACG possesses potent antitumor activity against human tumor xenografts in BALB/c *nu*/*nu* nude mice but not for tumors implanted in NOD/SCID mice deficient in macrophages and neutrophils, suggesting that these cells play an important role in activating 9ACG in the tumor microenvironment. Most importantly, antiangiogenic monoclonal antibody DC101 potentiated single-dose 9ACG antitumor activity and prolonged survival of mice bearing resistant human colon tumor xenografts by providing strong β-glucuronidase activity and prodrug delivery through enhancing inflammatory cell infiltration and normalizing tumor vessels in the tumor microenvironment. We also show that inflammatory cells (neutrophils) were highly infiltrated in advanced human colon cancer tissues compared with normal counterparts.

Conclusions: Our study provides *in vivo* evidence that 9ACG has potential for prodrug monotherapy or in combination with antiangiognesis treatment for tumors with infiltration of macrophage or neutrophil inflammatory cells.

Growing evidence indicates that diverse deregulated nonmalignant cells in the tumor microenvironment, in addition to malignant cells, can be crucial for carcinogenesis. The tumor microenvironment contains a complex system of many nonmalignant cell types, including endothelial cells, fibroblasts, and lymphocyte, neutrophil, and macrophage inflammatory cells. All of these cells coordinate with malignant cells and participate in tumor progression. It is generally thought that the function of the recruitment of neutrophils and macrophages is to reject the tumor. However, the tumor microenvironment can educate the neutrophils and macrophages to be immunosuppressive and contribute to carcinogenesis, a process termed immunoediting (1).

The presence of neutrophils and macrophages at the tumor site represents one of the hallmarks of cancer-associated inflammation (2–4). In patients with various types of cancer, the presence of increased numbers of tumor-infiltrating neutrophils or macrophages has been linked to poorer outcomes (5, 6). Neutrophils and macrophages, either acting alone or orchestrating together, contribute to tumor progression by producing several factors that enhance angiogenesis and remodeling of the extracellular matrix (7–9). Angiogenic factors secreted by tumor-associated macrophages include vascular endothelial growth factor, platelet-derived growth factor, interleukin 1, interleukin 8, β-fibroblast growth factor, tumor necrosis factor-α, and matrix metalloproteinase 9 (10). Some of these angiogenic factors act on the CXCR2 receptor

Authors' Affiliations: [1]Divisions of Urology and [2]Colon and Rectum, Departments of Surgery and [3]Pathology, Tri-Service General Hospital, and [4]Graduate Institute of Life Sciences and [5]Department of Biochemistry, National Defense Medical Center; [6]Institute of Biomedical Sciences, Academia Sinica; [7]Department of Microbiology and Immunology, National Yang-Ming University, Taipei, Taiwan; and [8]Department of Pharmacy, Chia Nan University of Pharmacy and Science, Tainan, Taiwan

Received 1/15/09; revised 3/31/09; accepted 3/31/09; published OnlineFirst 7/7/09.

Grant support: National Health Research Institutes grant NHRI-EX94-9420B1 (S.R. Roffler), and National Science Council grant NSC95-2314-B-016-028 and Department of Defense grants DOD97-28-01 and DOD97-28-02 (T-L. Cha).

The costs of publication of this article were defrayed in part by the payment of page charges. This article must therefore be hereby marked *advertisement* in accordance with 18 U.S.C. Section 1734 solely to indicate this fact.

Requests for reprints: Tai-Lung Cha, Tri-Service General Hospital and National Defense Medical Center, Number 325, Section 2, Chenggong Road, Neihu District, Taipei 114, Taiwan. Phone: 886-2-87923100, ext. 19391; Fax: 886-2-87927386; E-mail: tlcha@ndmctsgh.edu.tw and Steve R. Roffler, Institute of Biomedical Sciences, Academia Sinica, No. 128, Section 2, Academia Road, Taipei 11529, Taiwan; E-mail: sroff@ibms.sinica.edu.tw.

doi:10.1158/1078-0432.CCR-09-0090

Translational Relevance

Many glucuronide prodrugs have been developed to improve bioavailability and to overcome dose-related systemic toxicity. However, there are two major obstacles upon application of the prodrug for the treatment of cancer: (*a*) how to thoroughly activate the prodrug, and (*b*) how to deliver sufficient quantities of the prodrug into the tumor microenvironment. Our study showed that a novel cell-impermeable, nontoxic glucuronide prodrug, 9-aminocamptothecin glucuronide (9ACG), displays potent antitumor activity after activation by extracellular β-glucuronidase provided by neutrophils and macrophages in the tumor microenvironment. Most importantly, for prodrug-resistant tumors with scarce β-glucuronidase activity, the antiangiogenic monoclonal antibody DC101 enhances neutrophil and macrophage infiltration, and normalizes tumor vessels to activate 9ACG. Combined therapy with DC101 and a single dose of 9ACG suppressed resistant colon tumor growth and prolonged long-term survival of mice. Our study provides *in vivo* evidence that the 9ACG prodrug has potential for prodrug monotherapy or in combination with antiangiognesis treatment for clinical translation.

involved in the neutrophil-dependent proangiogenic cascade leading to endothelial cell invasion and vessel formation (11–13). In addition to proangiogenic factors, tumor-infiltrating neutrophils and macrophages also produce proteolytic enzymes, such as matrix metalloproteinase 2, matrix metalloproteinase 9, and β-glucuronidase (βG) to promote angiogenesis and tumor progression. The hypoxic and low-pH tumor microenvironment can up-regulate proteolytic enzyme expression and enhance their enzymatic activities (14). It has been known for a long time that βG is present mainly in the extracellular space of solid necrotic tumors (15–18). This provides a rationale to target the tumor microenvironment and develop nontoxic prodrugs selectively detoxified by a glucuronic acid moiety.

Tumor growth requires neoangiogenesis. However, tumor vessels are structurally and functionally abnormal, which creates a chaotic tumor microenvironment with severe hypoxia and necrosis, resulting in neutrophil and macrophage infiltration. In addition, the altered tumor vasculature impedes effective drug delivery and distribution into the tumor microenvironment (19). Abnormal tumor vessels with high vascular permeability combined with vascular resistance cause elevated interstitial fluid pressure in the tumor, which compromises the therapeutic efficacy of drugs (20, 21). Much effort has been devoted to investigating whether antiangiogenesis therapy can cause tumor vessel normalization to help drug delivery (22–26). Antiangiogenesis therapy with an antibody (bevacizumab) against vascular endothelial growth factor reduces microvascular density, vascular volume, and interstitial fluid pressure concurrent with increased uptake of a radioactive tracer in tumors, which suggests tumor vasculature was normalized and more efficient in delivering these agents to tumor parenchyma than before bevacizumab treatment in rectal cancer patients (27). A recent study also identified the onset and duration of a vascular normalization window created by an antiangiogenic agent, AZD2171, against vascular endothelial growth factor receptors in human glioblastoma patients, which provides insight that the timing of combined antiangiogenic and cytotoxic therapy may be critical for optimizing their therapeutic efficacy (28).

Although antiangiogenic therapy may potentiate the cytotoxic efficacy of chemotherapeutic agents, one of the major issues of chemotherapy in cancer treatment is the lack of tumor specificity, which leads to intolerable toxicity. Some strategies to overcome this deficit make use of nontoxic prodrugs that are selectively activated in the tumor microenvironment by enzymes, which liberate the toxin from the prodrug (29). βG is a lysozyme secreted by neutrophils and macrophages, and activated by a low pH value at the tumor microenvironment, which makes it a perfect target for the design of a nontoxic prodrug with a glucuronic acid moiety. 9-Aminocamptothecin, a camptothecin derivative, is a DNA topoisomerase I inhibitor (30, 31) that possesses remarkable activity against several cancer cell lines *in vitro* and antitumor effects in animal tumor models (32, 33). However, 9-aminocamptothecin has shown poor therapeutic effects for cancer patients in clinical trials (34). One important reason for the poor clinical trial result is the interaction of 9-aminocamptothecin with human serum albumin (35). We have developed 9-aminocamptothecin glucuronide (9ACG), a prodrug of 9-aminocamptothecin, that is highly water-soluble, exhibits low human serum albumin binding, and displays potent antitumor activity against human tumor xenografts in nude mice (36, 37).

In the present study, we found that 9ACG was nontoxic for various cancer cell lines *in vitro*. Only extracellular but not intracellular βG in cancer cells can activate 9ACG into 9-aminocamptothecin and show potent cytotoxicity. In addition, 9ACG possesses potent antitumor activity against human tumor xenografts in mice. This potent antitumor activity was dramatically lost in NOD/SCID mice with deficient macrophages and neutrophils, which suggests that the inflammatory cells (neutrophils and macrophages) play a role in activating 9ACG in the tumor microenvironment. Antiangiogenic monoclonal antibody (mAb) DC101 normalized the tumor vasculature and enhanced drug delivery into a tumor in a mice animal model. Pretreatment with DC101 by an optimal schedule potentiated the antitumor activity of a single dose of 9ACG and prolonged the survival of mice bearing resistant human colon tumor xenografts by increasing inflammatory cell infiltration and necrosis of the colon tumor. We also show that inflammatory cells (neutrophils) were highly infiltrated in advanced human colon cancer tissues compared with their normal counterparts. Our study provides *in vivo* evidence that the glucuronide prodrug 9ACG has potential for prodrug monotherapy or in combination with antiangiogenesis treatment for cancer therapy, especially for those tumors infiltrated with macrophage or neutrophil inflammatory cells.

Materials and Methods

Mice. Female NOD/SCID mice were bred at the Institute of Biomedical Sciences (Taipei, Taiwan). Female BALB/c *nu/nu* mice were purchased from the National Laboratory Animal Breeding and Research Center. Female SCID-Beige (C.B17 scid/Beige) mice were purchased from the Laboratory Animal Center, National Taiwan University College of Medicine. Nude mice are deficient in T cells and possess

low B-cell function but have high natural killer cell activity; SCID-Beige mice have deficiencies in T, B, and natural killer cells, whereas NOD/SCID mice are deficient in T cells, B cells, natural killer cells, and macrophages, and display multiple defects in innate immunity. The backgrounds of immunodeficient mouse strains are described in the supplementary materials. All experiments were conducted in accordance with institutional guidelines for animal care and use.

Antibodies. DC101 hybridoma cells were obtained from the American Type Culture Collection (ATCC). The DC101 hybridoma was cultured in a CELLine 1000 system (BD Biosciences). DC101 in the culture supernatant was purified by affinity chromatography on Protein A Sepharose (GE Healthcare Bio-Sciences Corp.). Rat anti-mouse CD31 (clone MEC13.3), rat anti-mouse Gr-1 (clone RB6-8C5), and rat control IgG2b antibodies were from BioLegend. Rat anti-mouse CD68 (clone FA-11) and rat anti-mouse F4/80 (clone CI:A3-1) were from AbD Serotec. Rabbit anti-asialo GM1 was from Wako Chemicals. Goat anti-rat IgG-biotin and avidin–horseradish peroxidase were from MP Biomedicals. Goat anti-rabbit IgG-biotin was from Chemicon. Mouse anti-human CD68 (clone KP1) and polyclonal rabbit anti-human myeloperoxidase (for human granulocytes) were from Dako.

Cell lines. Murine MPS VII skin fibroblasts (3,521; βG deficient) and 3,522 fibroblasts (normal βG levels) isolated from heterozygous mouse (38) cells, kindly provided by Mark Sands, Washington University, School of Medicine, St. Louis, MO, were cultured in DMEM (4.5 g/L glucose) supplemented with 10% bovine serum, 2.98 g/L HEPES, 2 g/L $NaHCO_3$, 100 units/mL penicillin, and 100 μg/mL streptomycin. CL1-5 human lung adenocarcinoma, kindly provided by Dr. Pan-Chyr Yang from the Institute of Biomedical Sciences, Taipei, Taiwan, LS-174T human colorectal adenocarcinoma (ATCC CL-188), HT29 human colon carcinoma (ATCC HTB-38), PLC/PRF/5 human hepatocarcinoma (ATCC CRL-8024), EJ human bladder cancer, BT-20 human breast carcinoma (ATCC HTB-19), and HepG2 human hepatocarcinoma (ATCC HB-8065) cells were cultured in RPMI containing the same supplements in a 5% CO_2-humidified atmosphere. Cells were routinely tested for mycoplasma with a Rapid Detection kit according to the manufacturer's instructions (Gen-Probe).

CL1-5 cells expressing cytosolic βG. CL1-5 cells were transfected with pNeo/GUS (39), which codes for the full-length eβG (*Escherichia coli* βG) gene. Cells were selected in medium containing 0.5 mg/mL G418, and whole cell lysates prepared from single clones were screened for βG activity to isolate CL1-5/c-eβG cells.

CL1-5 cells expressing membrane-tethered βG. pLNCX-mβG-e-B7, which codes for a membrane-tethered form of murine βG on cells (28), was cotransfected with pVSV-G (Clontech) into GP293 cells (Clontech) to produce recombinant retroviral particles. Two days after transfection, the culture medium was filtered, mixed with 8 mg/mL polybrene, and added to CL1-5 lung cancer cells. Stable cell lines were selected in medium containing 0.5 mg/mL G418 (Calbiochem). Single colonies expressing moderate (CL1-5/s-mβG^{med}) or high (CL1-5/s-mβG^{hi}) levels of murine βG on their surface were isolated by limiting dilution cloning combined with flow cytometric analysis of murine βG surface expression.

Flow cytometric assay. CL1-5, CL1-5/s-mβG^{med}, and CL1-5/s-mβG^{hi} cells were subjected to indirect immunofluorescence staining for the expression of surface mouse βG with the use of rat mAb 7G7 against mouse βG (28). Cells (10^6) were incubated with 5 μg/mL 7G7 in 0.5% bovine serum albumin/PBS for 1 h on ice. The cells were washed twice, and FITC-conjugated goat anti-rat Ig (1:1,000; ICN Pharmaceuticals) was added at 4°C for 1 h. The cells were then washed with ice-cold PBS, suspended in PBS containing 5 μg/mL propidium iodide (Sigma), and passed through a 40-μm nylon filter (Falcon 2340) to remove cell aggregates before analyzing fluorescence intensity on a FACSCaliber flow cytometer (Becton Dickinson). Data was analyzed with FlowJo 3.2 (Tree Star Inc.).

In vitro *cytotoxic assay.* Defined concentrations of 9-aminocamptothecin or 9ACG were added to cells in 200 μL complete medium at pH 6.8 for 24 h. The cells were washed and incubated in fresh medium for 24 h and then pulsed for 16 h with ^{3}H-thymidine (1 μCi/well). The cells were harvested, and radioactivity was measured in a TopCount Microplate Scintillation Counter (Packard). Results are expressed as percent inhibition of ^{3}H-thymidine incorporation into cellular DNA compared with untreated cells.

Cellular βG activity. Cells at 90% confluence were washed twice with PBS and then suspended on ice for 30 min in PBS/0.1% Tween 20. Cells were broken on a mechanical dounce, and the cell supernatant was clarified by centrifugation at 10,000 × g for 20 min at 4°C. The enzymatic activity of βG was measured in triplicate by incubating 20 μL cell lysate, 10 μL 3.5 mmol/L 4-methylumbelliferyl β-D-glucuronide, and 70 μL reaction buffer (50 mmol/L bis-TRIS, 50 mmol/L triethanol amine, 100 mmol/L acetic acid, 0.1% bovine serum albumin) in a microtiter plate for 60 min at 37°C. The reaction was quenched by adding 120 μL 0.5 M $NaHCO_3$, and fluorescence was measured at excitation/emission wavelengths of 355/460 nm in a microplate spectrofluorometer. Specific enzymatic activities are expressed in nanomoles of released 4-methylumbelliferone (MU) per milligram of protein per hour (nmol 4-methylumbelliferone (MU) mg^{-1} h^{-1}).

Xenograft mouse model. Wild-type LS174T cells were s.c. injected in the right flank of 8-wk-old female BALB/c *nu/nu* mice or NOD/SCID mice. Mice bearing 200 to 300 mm^3 tumors were i.p. injected every 3 d with 800 μg DC101 or 800 μg isotype-matched control rat IgG1. After three injections of DC101, mice were i.v. injected with 50 mg/mg 9ACG and then injected once more with DC101 antibody 3 d later. Tumor growth was measured with calipers every 3 d, and the tumor volume was estimated at 0.5 × height × width × length. Mice were killed on day 125, and tumors were harvested for immunohistochemistry of late-phase tumors.

In an early–time phase experiment, to begin investigating tumor morphology and immune cells at earlier times after drug treatment, immunohistochemistry was done on LS174T tumors on day 0 after the mice had received DC101 antibody treatment on days -6 and -3 (to determine the tumor microenvironment when the prodrug was given), or on days 3 and 7 after the mice had received the DC101 antibody on days -6, -3, and 0, and 50 mg/kg 9ACG on day 0. Mice treated with PBS on days -6 and -3 were included as a control. The sections were stained for H&E, collagen, CD31 (blood vessels), macrophages, granulocytes, and natural killer cells. The time course of this experiment is described in the supplementary materials.

Immunohistochemical analyses. Tissue sections were fixed in cold acetone, followed by 4% paraformaldehyde. Specimens were then incubated with 3% H_2O_2 in PBS for 15 min at room temperature to block endogenous peroxidase. Rat anti-CD31 antibody was diluted 1:200 in protein-blocking solution and applied to the sections overnight at 4°C. Biotin-conjugated goat anti-rat IgG was diluted 1:200. After incubating with the secondary antibody for 1 h at room temperature, the samples were washed and incubated with 3-amino-9-ethylcarbazole (AEC) substrate (Zymed). Staining was monitored under a bright-field microscope, and the reaction was stopped by washing with distilled water. Sections were counterstained with hematoxylin (Sigma-Aldrich) and mounted overnight with Universal Mount (Research Genetics). Treatment procedures for control specimens were similar except that the primary antibody was omitted. For H&E staining, sections were deparaffinized in xylene followed by 100%, 95%, and 80% ethanol washes, and then rehydrated in PBS (pH 7.5). Continuous tumor cryosections were stained for βG activity with X-GlcA (Sigma-Aldrich) and counterstained with nuclear fast red. X-GlcA was applied to tissue sections in phosphate buffer (pH 4.5) containing potassium ferricyanide and potassium ferrocyanide. The amount of intratumor collagen was quantified through image analysis of Sirius red–stained tumor sections as well as by quantifying hydroxyproline content. Quantitative analysis of collagen was done by morphometric analysis. The total amount of collagen stained on each submitted section was calculated by a computer via the digitalized image. The sections

were examined on an upright BX4 microscope (Olympus) or viewed in phase contrast and fluorescence modes on an inverted Axiovert 200 microscope (Carl Zeiss Microimaging).

Pharmacokinetics in tumors. Four groups of three mice bearing established LS174T tumors were i.p. injected with 800 μg DC101 every 3 d for 4 cycles. 4-Methylumbelliferyl β-D-glucuronide hydrate dissolved in PBS at a concentration of 5 mg/mL was i.v. injected (25 mg/kg) through the tail veil 3 d after each round of DC101 treatment in one group of mice. Mice receiving 4-methylumbelliferyl β-D-glucuronide were sacrificed 15 min later, and their tumors were weighed and immediately preserved in liquid nitrogen. Tumors were homogenized for 1 min on ice in homogenization buffer (50% MeOH, 20 mmol/L phosphate buffer, and 1 mmol/L saccharolactone). Proteins were precipitated with 50 mmol/L trichloroacetic acid before the crude lysates were briefly centrifuged at 3,000 rpm to remove large debris, further centrifuged at 14,000 rpm for 20 min at 4°C, and then subjected to high performance liquid chromatography (HPLC) analysis. A scheme showing the time course of this experiment is provided in the supplementary materials.

HPLC analysis. Reversed-phase high performance liquid chromatography determination of 4-methylumbelliferyl β-D-glucuronide was done with the use of a mobile phase of 50% methanol in 5 mmol/L phosphate buffer (pH 6.5) at 1 mL/min in a 150 × 3.9 mm Nova-Pak column (Waters). A Jasco spectrofluorometer operated at 375 nm excitation and 460 nm emission was used to record spectra.

Statistics. Comparisons were made with the use of unpaired two-tailed Student's *t* tests assuming unequal variance done with the use of the analysis programs SigmaPlot and SigmaStats.

Results

9ACG activation is independent of the levels of endogenous βG. The enzyme activity of βG is required for the conversion of the prodrug 9ACG into the active form 9-aminocamptothecin. We first investigated whether intracellular βG activity was involved in 9ACG cytotoxicity in cancer cell lines. The cytotoxic sensitivity of a panel of tumor cells to the prodrug 9ACG and its active form 9-aminocamptothecin, and the βG activity present in homogenates prepared from these cells were examined. The specific βG activities of seven cancer cell lines ranged from 85 units/mg protein for LS174T cells to <20 units/mg protein for HT-29 cells (one unit of activity corresponds to the hydrolysis of

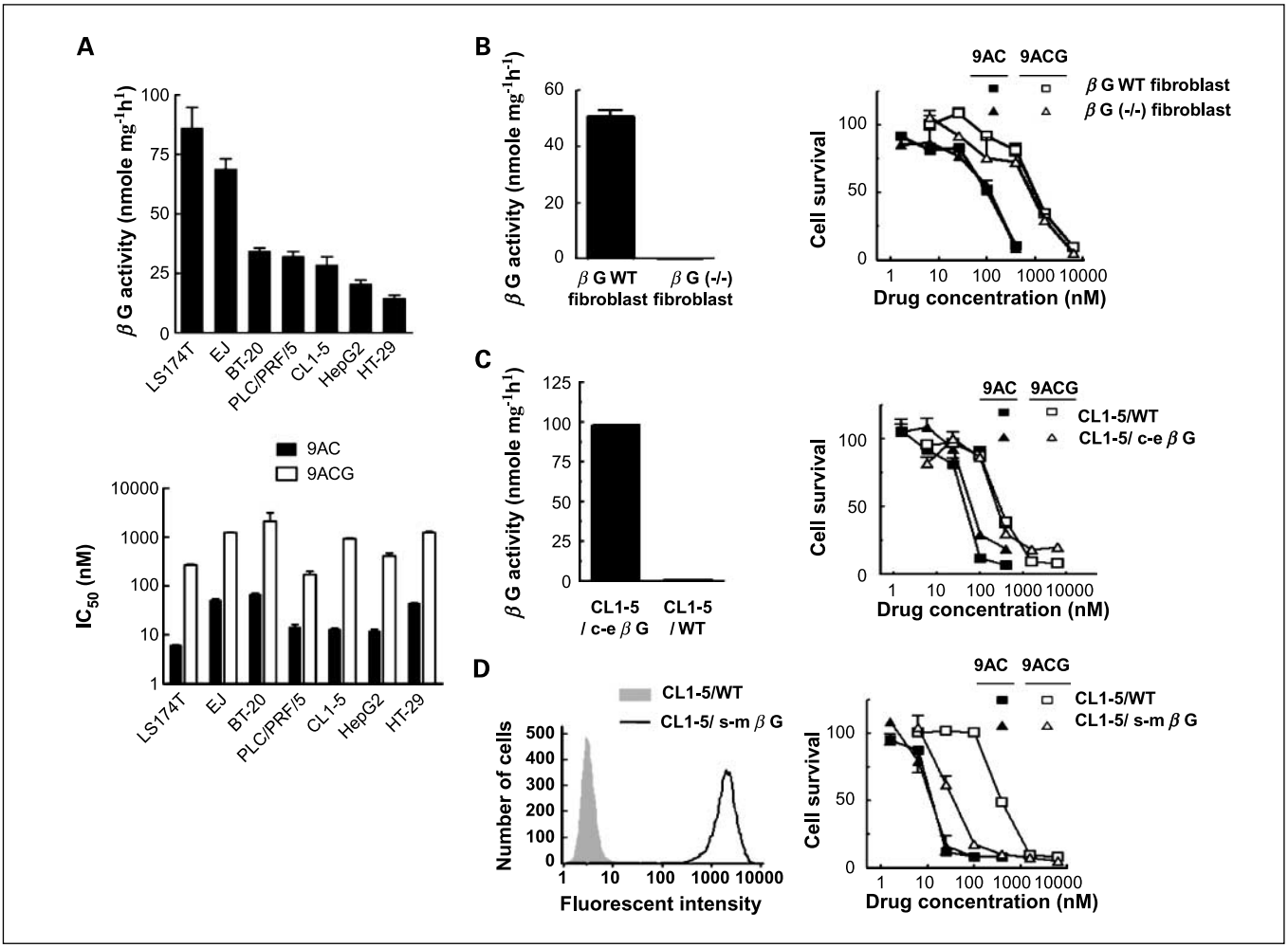

Fig. 1. Extracellular βG activates 9ACG. *A,* βG activity of cell lysates prepared from cancer cell lines (*top*), determined by measuring the fluorescence generated through hydrolysis of MU β-D-glucuronide (MUG). Bottom, cells were exposed to 9-aminocamptothecin or 9ACG for 24 h, and then incubated in fresh medium for 24 h more before ^{3}H-thymidine incorporation was measured. Half maximal inhibitory concentration values were determined by interpolation of inhibition curves. Results, mean of triplicates ± SE. *B,* βG activity of MPS VII βG-deficient fibroblasts and βG-positive fibroblasts (*left*), measured as described in (*A*). Right, drug sensitivity measured by ^{3}H-thymidine incorporation. *C,* βG activity at pH 7.0 of CL1-5 cells or eβG-expressing CL1-5 cells (*left*). Right, drug sensitivity measured by ^{3}H-thymidine incorporation. *D,* surface expression levels of wild-type and CL1-5 cells expressing membrane-tethered mβG (*left*; CL1-5/s-mβG). Right, drug sensitivity measured by ^{3}H-thymidine incorporation.

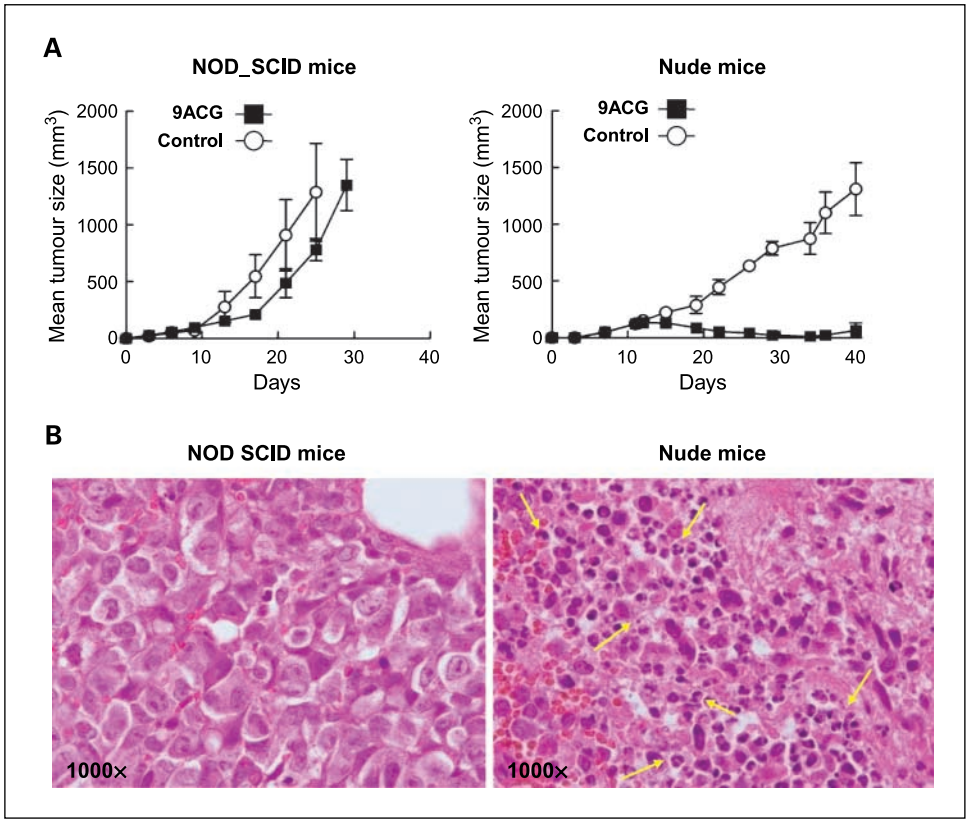

Fig. 2. 9ACG antitumor activity depends on innate immune cells. *A,* NOD/SCID mice and BALB/c *nu/nu* mice were s.c. inoculated with CL1-5 human lung cancer cells in the right flank. Tumor-bearing mice were i.v. injected with 50 mg/kg 9ACG or PBS (as control) on day 11 after the tumor cells were inoculated, and tumor volumes were measured. *B,* H&E-stained tumor sections showing that the innate immune cells were highly infiltrated in tumors from nude mice. Arrows, tumor-infiltrating granulocytes.

1 nmol substrate in 1 h; Fig. 1A, *top*). There was no correlation between the endogenous βG activity and cytotoxic sensitivity to 9ACG among these seven cancer cell lines (Fig. 1A, *bottom*), suggesting that the intracellular endogenous βG activity of the cancer cell itself is not a determinant of 9ACG activation.

To verify whether or not intracellular βG activity could activate 9ACG, we examined the drug sensitivity of 9ACG to wild-type and βG-deficient fibroblasts. Fibroblasts (3,521) were derived from βG knockout MPS VII mice, whereas 3,522 fibroblasts came from a matched heterozygous littermate. The 3,521 $\beta G^{(-/-)}$ fibroblasts contained <1 unit/mg protein βG activity, whereas the 3,522 fibroblasts had about 50 units/mg protein βG activity (Fig. 1B, *left*). 9ACG was relatively nontoxic to both wild-type and βG-deficient fibroblasts (Fig. 1B, *right*). We also generated CL1-5 lung cancer cells (CL1-5/c-eβG) that stably expressed eβG (derived from *E. coli* with high βG activity) in its cytosol (Fig. 1C, *left*), and CL1-5/s-mβG cells with mouse βG (relatively low activity) tethered to the cell surface (Fig. 1D, *left*). Only CL1-5/s-mβG cells were more sensitive to 9ACG compared with parental CL1-5 cells (Fig. 1D, *right*), suggesting that extracellular βG was responsible for prodrug activation. We further investigated the drug uptake rate of 9-aminocamptothecin and 9ACG in tumor cells by high performance liquid chromatography. The intracellular levels of 9-aminocamptothecin reached a plateau within 1 minute with similar uptake kinetics at 4°C and 37°C, suggesting that 9-aminocamptothecin passively diffused through the cellular membrane into the cells (data not shown). In contrast, the intracellular 9ACG could not be detected over a period of 30 minutes. Taken together, these results clearly showed that 9ACG is cell-impermeable, and the intracellular endogenous βG activity of the cancer cell itself should not be a determinant of the cell-impermeable prodrug 9ACG activation. Hence, there must be other sources that provide βG to activate 9ACG in the tumor microenvironment.

Neutrophils and macrophages are involved in the activation of 9ACG prodrug. A previous article showed that βG was liberated extracellularly with a high local concentration by neutrophils and macrophages in necrotic tumor areas (40). We used two xenograft models, BALB/c *nu/nu* nude and NOD/SCID mice, with or without mature innate immune cells to examine whether the infiltrated innate immune cells in a tumor microenvironment contribute to 9ACG prodrug activation *in vivo*. CL1-5 lung cancer cells were s.c. injected into NOD/SCID and nude mice. When tumors had grown to 200 mm^3, one single i.v. injection of either 50 mg/kg 9ACG or PBS was given. Interestingly, one single 9ACG therapy completely suppressed CL1-5 tumor growth in BALB/c *nu/nu* nude mice, but NOD/SCID mice bearing CL1-5 tumors failed to respond to 9ACG *in vivo* (Fig. 2A). Immunohistochemical staining clearly showed that innate immune cells were highly infiltrated in the BALB/c *nu/nu* nude mice bearing CL1-5 tumors but were barely present in tumors derived from NOD/SCID mice (Fig. 2B). These results suggested that innate immune cells, such as neutrophils and macrophages, may provide extracellular βG to activate the 9ACG prodrug in the tumor microenvironment and suppress tumor growth through bystander effects.

DC101 enhances inflammatory cell infiltration and βG enzyme activity in the tumor microenvironment. Because the prodrug 9ACG is cell-impermeable, its *in vivo* antitumor activity depends on two major issues in the tumor microenvironment: (*a*) essential βG enzyme activity for prodrug activation, and (*b*)

an adequate delivery system for prodrug accumulation. In contrast to CL1-5 human lung cancer cells, which could be cured by 9ACG monotherapy, LS174 human colorectal cancer cells are more resistant to 9ACG treatment in our xenograft model (36). We wondered whether inflammatory cell infiltration was insufficient to provide adequate βG enzyme activity for 9ACG prodrug activation in the resistant LS174 tumor microenvironment. To test the hypothesis that antiangiogenesis treatment may enhance inflammatory cell infiltration and accelerate 9ACG prodrug activation in the resistant LS174 tumor microenvironment, we treated BALB/c *nu/nu* mice bearing established LS174T tumors with anti–vascular endothelial growth factor receptor 2 mAb (DC101 mAb) followed by a single 50-mg 9ACG i.v. injection as well as individual treatments of DC101 mAb alone or vehicle (PBS) alone. The neutrophil and macrophage infiltration, and tumor necrosis were examined by immunohistochemical staining in LS174T tumors after the mice had received PBS on days -6 and -3, and observed on day 0 (Day 0 Control); DC101 mAb on days -6 and -3 with observation on day 0 (Day 0 DC101); or combined therapy with DC101 mAb on days -6, -3, and 0, and 9ACG on day 0, with observation on day 3 (Day 3 DC101/9ACG). As expected for this resistant tumor, the neutrophil and macrophage infiltration was low in the control group (Fig. 3A). Interestingly, DC101 mAb treatment resulted in a dramatic increase of both neutrophil and macrophage infiltration, and their βG enzyme activities in the tumor microenvironment (Fig. 3B and C). 9ACG i.v. administration resulted in decreased DC101-induced neutrophil and macrophage infiltration, which suggested that the 9ACG prodrug was activated and induced cellular destruction in the resistant LS174 tumor microenvironment. A terminal deoxyribonucleotide transferase–mediated

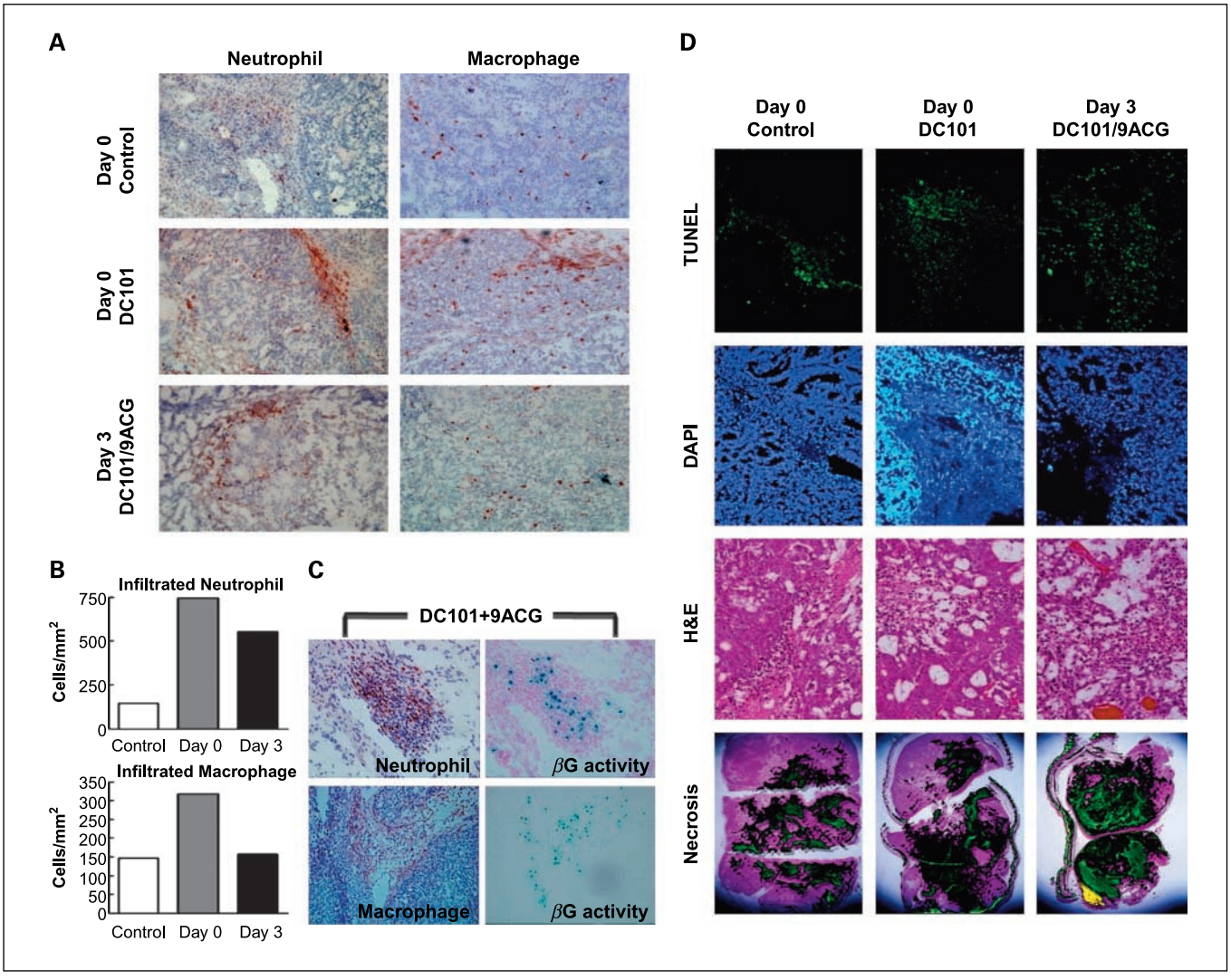

Fig. 3. DC101 enhances neutrophil and macrophage infiltration and promotes 9ACG activation in prodrug-resistant LS174T tumors. *A,* BALB/c *nu/nu* mice bearing 9ACG-resistant LS174T tumors were treated on days -6 and -3 with PBS (Day 0 Control); with i.p. injections of DC101 on days -6 and -3, observed on day 0 (Day 0 DC101); or with i.p. injections of DC101 on days -6, -3, and 0, and one i.v injection of 50 mg/kg 9ACG on day 0, observed on day 3 (Day 3 DC101/9ACG). Tumor sections were stained with anti–Gr-1 and anti-CD68 antibodies for neutrophils and macrophages, respectively. *B,* neutrophil and macrophage infiltration. Data, quantification of six independent microscopy fields at ×200 magnification. *C,* comparative studies by enzyme histochemistry showed neutrophils and macrophages with high βG enzyme activity infiltrated into LS174T tumors treated with DC101 and 9ACG. *D,* TUNEL analysis of tumor tissues showed marked apoptosis from mice treated with DC101 plus 9ACG compared with treatment with PBS (control) or DC101 alone. Tumor necrosis showed the same tendency as the TUNEL assay, which was shown by the presence of green fluorescence in H&E-stained sections resulting from the aforementioned treatments. TUNEL, terminal deoxyribonucleotide transferase–mediated nick-end labeling.

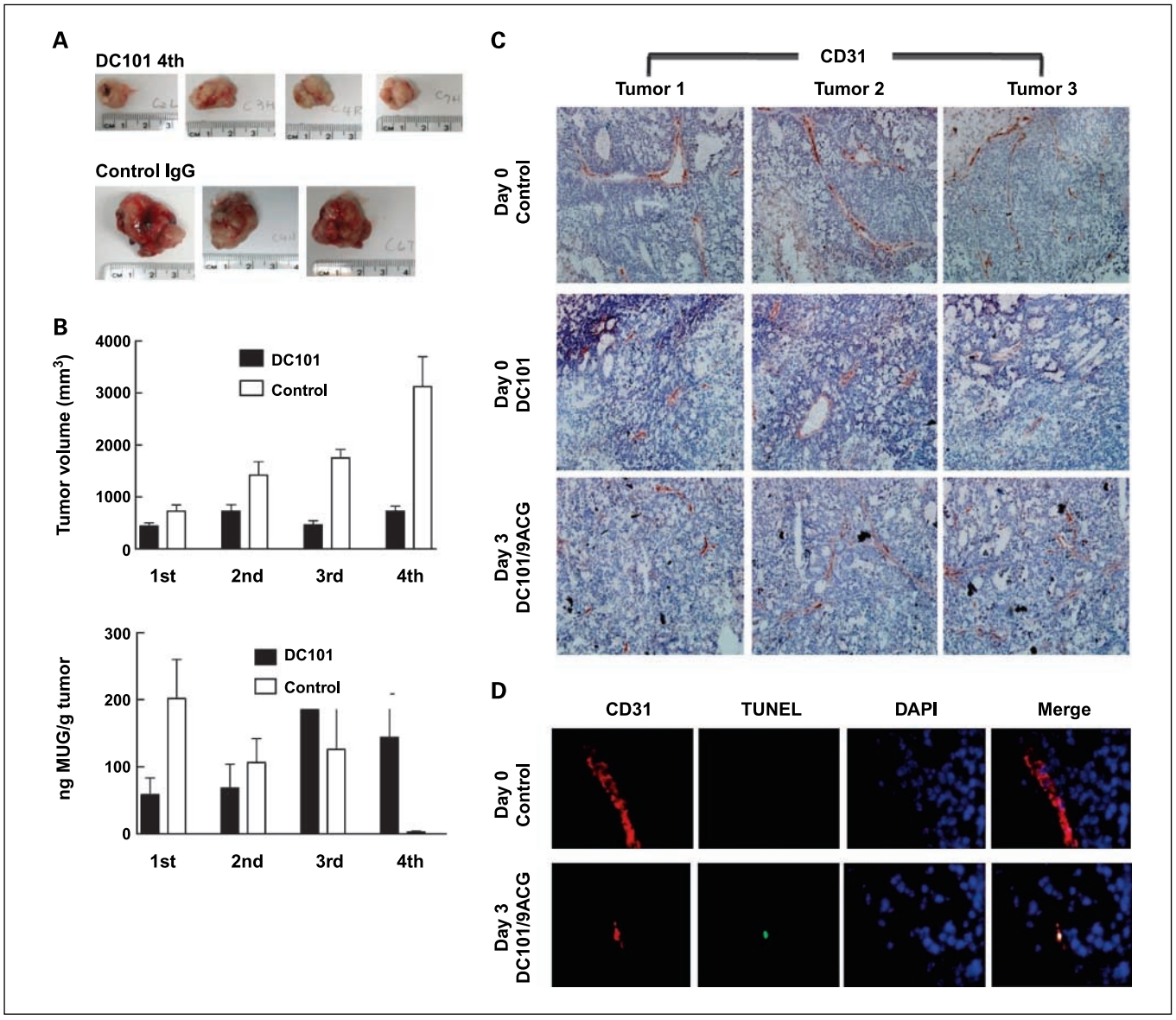

Fig. 4. DC101 promotes prodrug delivery into prodrug-resistant LS174T tumors. *A,* LS174T tumors removed from SCID-Beige mice after 4 cycles of DC101 or control antibody given every 3 d. *B,* tumor size (*top*) and HPLC analysis (*bottom*) of MUG accumulation in tumors 15 min after i.v. injection of MUG to mice bearing LS174T xenografts. MUG was injected immediately after DC101 or control antibody injection at the indicated treatment cycles. Data, mean ± SE. *C,* representative sections showing CD31 staining at ×200 magnification of tumors from mice treated with PBS control, DC101 every 3 d for 3 cycles, and DC101 every 3 d for 3 cycles plus 9ACG. *D,* fluorescent image of a tumor section showing endothelial cells (*red*, stained with fluorescein-conjugated anti-CD31 mAb), apoptotic cells (*green*, stained with TUNEL), and nuclei (*blue*, stained with 4,6-diamidino-2-phenylindole). DC101 + 9ACG treatment led to significant apoptosis of vascular endothelial cells, which was notably absent in the control groups.

nick-end labeling assay and immunohistochemical staining both showed profound cell apoptosis and tissue necrosis in mice bearing tumors under DC101 and 9ACG combined therapy (Fig. 3D).

DC101 normalized tumor vessels and promoted prodrug delivery in the tumor microenvironment. Our previous results indicated that antiangiogenesis treatment enhanced inflammatory cell infiltration and provided βG enzyme activity to potentiate 9ACG prodrug activation in a resistant tumor microenvironment. To further test the hypothesis that antiangiogenesis therapy may normalize tumor vessels and enhance the therapeutic efficacy of 9ACG, we designed experiments to determine the optimal drug delivery schedule for combining 9ACG with antiangiogenesis therapy. To avoid the 9ACG prodrug–induced toxic effect activated by βG of tumors, we used a nontoxic glucuronide drug, 4-methylumbelliferyl β-D-glucuronide, as a drug model to mimic 9ACG. We treated mice with 800 μg DC101 per mouse every 3 days after s.c. LS174 tumors had grown to 200 to ~300 mm^3 (Fig. 4A). During each combined treatment, one group of mice was i.v. injected with 4-methylumbelliferyl β-D-glucuronide immediately after DC101 mAb i.p. treatment, and the s.c. tumors were excised 15 minutes after drug delivery for HPLC analysis. In the control groups, although tumors gradually increased in size, the MUG drug delivery into the tumors decreased inversely. In mice under DC101 treatment, the tumors were relatively small, but

the MUG drug delivery into the tumors showed an increased tendency (Fig. 4B). Immunohistochemical staining also showed that the number and size of tumor vessels decreased in mice bearing tumors under DC101 treatment compared with the control group (Fig. 4C). DC101 treatment induced apoptosis of vascular endothelial cells, which may contribute to increased neutrophil and macrophage infiltration in the tumor microenvironment (Fig. 4D). Our data were consistent with a previous study (41) and support the finding that antiangiogenesis treatment can normalize tumor vessels to promote prodrug delivery and that the optimal schedule for prodrug delivery was immediately after the third DC101 mAb treatment in the resistant LS174 xenograft tumor model.

DC101 synergistically enhanced 9ACG tumor inhibition and mouse survival. After the aforementioned schedule, we treated BALB/c *nu/nu* mice bearing established LS174T tumors with DC101 mAb treatment thrice followed by a single 50-mg/kg 9ACG i.v. injection as well as individual treatments of 9ACG with control mAb, DC101 mAb alone, or vehicle (PBS) alone. As expected for this resistant tumor, treatment with 9ACG combined with the control antibody had little effect on tumor growth. Treatment of mice with DC101 mAb alone modestly delayed growth, but all tumors progressed. In contrast, long-term suppression of tumor growth was achieved in mice treated with three doses of DC101 mAb followed by one injection of 9ACG (Fig. 5A). Most importantly, combined treatment with

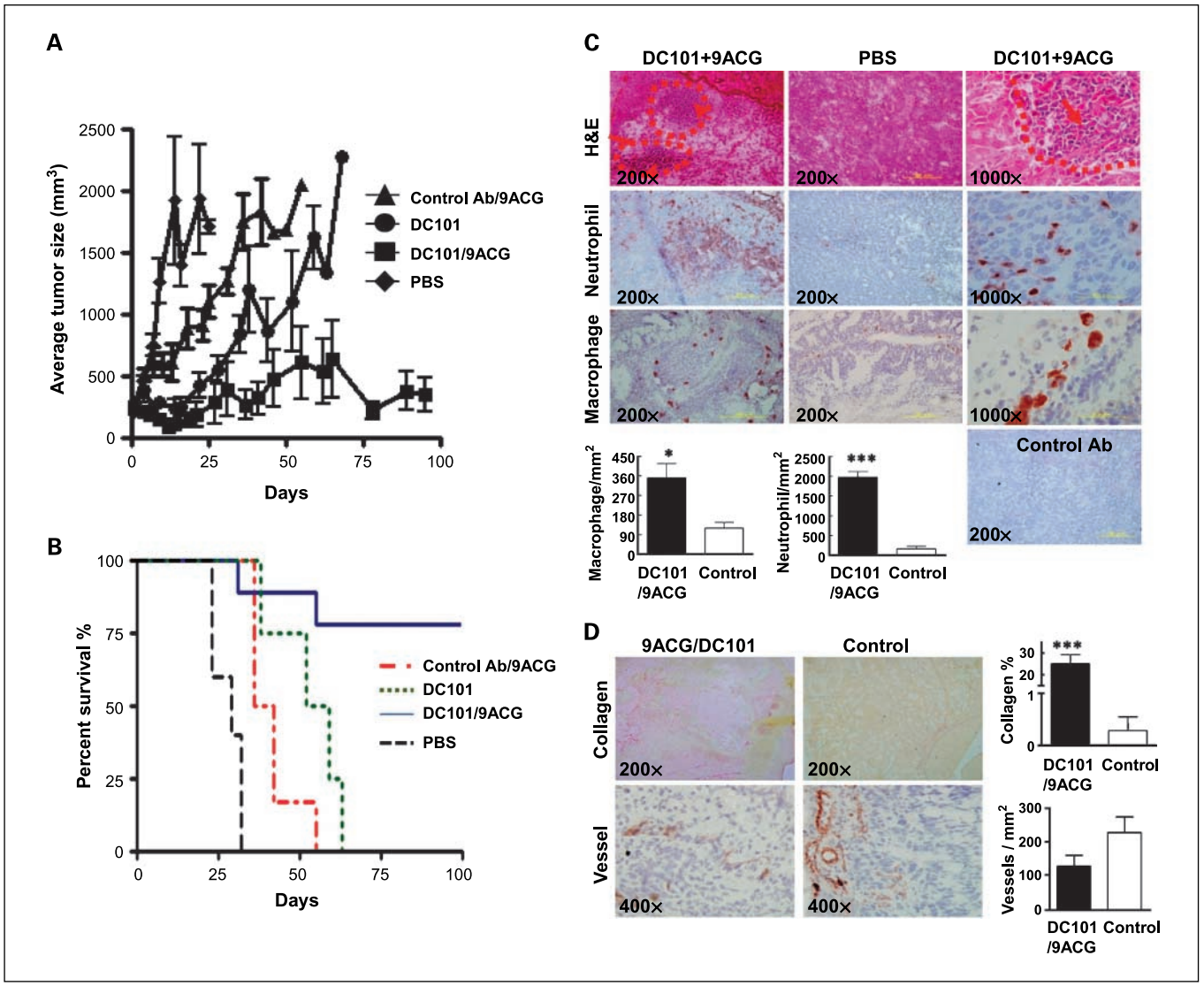

Fig. 5. DC101 synergizes 9ACG antitumor activity of prodrug-resistant LS174T tumors and prolongs mice survival. BALB/c *nu/nu* mice bearing 9ACG-resistant LS174T tumors were divided into four treatment groups. Mice in group 1 ($n = 6$) and group 2 ($n = 10$) were i.p injected with 800 μg control antibody or DC101 every 3 d for 4 cycles, and one i.v. injection of 50 mg/kg 9ACG after the 3rd cycle of DC101. Mice in group 3 ($n = 4$) were i.p injected with 800 μg DC101 every 3 d for 4 cycles, whereas mice in group 4 ($n = 5$) were i.p injected with PBS vehicle every 3 d for 4 cycles. *A,* the average tumor volume and (*B*) mouse survival are shown. *C,* BALB/c *nu/nu* mice bearing LS174T tumors treated with vehicle (PBS) alone, or DC101 and 9ACG as described above were sacrificed on day 125. Cryosection samples of day-125 tumors and size-matching LSI74T tumors were stained with H&E. The infiltrated neutrophils and macrophages were stained with anti – Gr-1 and anti-CD68 antibodies, and quantified by counting the neutrophils and macrophages under six independent microscopy fields at ×200 magnification, respectively. Bars, SE. *D,* fibrosis status and microvascular density in tumors treated as described above are shown by staining with sinus red and anti-CD31 antibody, respectively. Mean percentage of fibrotic area (collagen %) and number of vessels per square millimeter are shown. Bars, SE.

9ACG and DC101 mAb showed significant long-term survival of mice bearing drug-resistant LS174 human colorectal carcinoma tumors (Fig. 5B). These results indicate that antiangiogenesis treatment synergistically potentiated the 9ACG therapeutic efficacy. To further investigate the mechanisms of combined therapy with 9ACG and DC101 mAb responsible for long-term tumor inhibition, we used immunohistochemical staining to determine the morphologic changes and infiltrating immune cells in late-stage tumors (those remaining 125 days after combination therapy). S.c. LSI74T tumors were optimal cutting temperature–embedded, cryosectioned, and stained with H&E. Abundant innate immune cells, especially neutrophils and macrophages, infiltrated into LSI74T tumor tissues (Fig. 5C). The number of natural killer cells showed no difference in PBS-treated or combined-treated tumors (data not shown).

The significant accumulation of neutrophils and macrophages in tumors treated with 9ACG and DC101 mAb suggested that innate immunity may be involved in the long-term suppression of LS174T tumor growth. Fibrosis is commonly observed after immune-mediated tissue damage. We investigated the tissue fibrotic status in tumors under different combined treatments by immunostaining sinus red to visualize collagen formation. Tumors treated with the combined therapy displayed clearly abundant sinus red staining, indicating that an immune response occurred in those tumors (Fig. 5D). We then further quantified the innate immune cell infiltration, microvascular density, and fibrotic status in tumors between the combined-therapy and size-matched controls. The neutrophil and macrophage infiltration, and fibrosis were significantly higher in combined-treated tumors than in control tumors. The microvascular density in combined-treated tumors showed a decreased tendency, yet it did not reach statistical significance (Supplementary Table S5).

Neutrophil and macrophage infiltration in normal and colon cancer tissues. Because neutrophils and macrophages were the major players in activating the 9ACG prodrug in the tumor microenvironment in our colorectal cancer animal models, we wanted to check the neutrophil and macrophage infiltration status in human colorectal cancer tissues compared with their normal counterparts. Immunohistochemical analyses of archival human paraffin-embedded adenocarcinomas were done on randomly selected (16 pairs of colorectal cancers). Serial sections of samples of each tumor were stained for CD68, Gr-1, or human IgG. In all tumors studied, abundant Gr-1$^+$ neutrophils and CD68$^+$ macrophages were observed infiltrated in tumor tissues compared with their normal counterparts. In particular, the neutrophil infiltration in tumor tissues was highly statistically significant and about 10-fold higher in the tumor samples compared with their normal counterparts (Fig. 6A and B). These results clearly showed that innate immune cells were highly infiltrated in human colorectal cancer tissues and that they could serve as perfect targets for a clinical trial by using combined therapy with the 9ACG prodrug and antiangiogenesis in the near future.

Discussion

In this study, we showed that the glucuronide prodrug 9ACG has potential as a prodrug monotherapy or in combination with antiangiogenesis treatment for cancer therapy, especially for those tumors with a tumor microenvironment infiltrated with macrophage or neutrophil inflammatory cells. Our data showed that 9ACG, a cell-impermeable prodrug, could be extracellularly converted into the active form 9-aminocamptothecin by βG enzyme, which is mostly derived from neutrophils and macrophages that infiltrated into the tumor microenvironment. A combination with antiangiogenic agents, for example, anti–vascular endothelial growth factor receptor 2 DC101 mAb in this study, not only enhanced innate immune cell infiltration in the tumor microenvironment (which is required for the activation of the 9ACG prodrug) but also increased drug accumulation mediated through the normalization of tumor vasculatures in the tumors. Antiangiogenesis treatment is an attractive strategy to overcome two major obstacles upon application of prodrugs in the treatment of cancer: (*a*) how to thoroughly activate the prodrug, and (*b*) how to deliver sufficient quantities of the prodrug into the tumor microenvironment.

Although it is unclear whether inflammation is sufficient for the development of cancer, the connection between inflammation and cancer is now generally accepted. The hallmarks of cancer-related inflammation, including the presence of inflammatory cells and mediators, are present in the tumor microenvironment of most, if not all, tumors, irrespective of underlying triggers. The components of infiltrated inflammatory cells in the tumor microenvironment include neutrophils, macrophages, lymphocytes, and related cells, which provide various enzymes, including βG, that are involved in carcinogenesis and disease progression (42). This provides a rationale for the development of a prodrug targeting the inflammatory tumor microenvironment. Many glucuronide prodrugs have been developed to improve bioavailability and to overcome dose-related systemic toxicity (43, 44). Although βG is present in a variety of human tissues, problems with glucuronide prodrugs include their rapid clearance, predominant activation in inflammatory necrotic tumor areas, and lack of intracellular activation (44, 45). To overcome these limitations, antibody-directed enzyme prodrug therapy, gene-directed enzyme prodrug therapy, and virus-directed enzyme prodrug therapy approaches have been developed (46, 47). However, all of these approaches have been limited to date by several drawbacks, including the scarcity of tumor-specific antigens, adverse immune effects, and the need for penetration of the released drug through the cell membrane. A previous study has shown that antiangiogenesis treatment amplifies human T-cell activation through the induction of nuclear factor κB, nuclear factor of activated T cells, and activation protein 1 transcription factors (48). DC101 mAb has also been shown to induce T-cell–mediated antitumor immune responses leading to tumor rejection in the absence of immune tolerance; both CD4+ and CD8+ T cells contribute to this effect. In addition, DC101 treatment does not inhibit but improves T-cell infiltration into tumors (49). Our study showed that DC101 mAb treatment resulted in an increase of innate immune cells, especially neutrophil and macrophage infiltration in the tumor microenvironment, which provides adequate βG enzyme activity for prodrug activation. Therefore, antiangiogenesis treatment not only has an effect on the cellular immune system but also on the innate immune system to promote inflammatory cell infiltration into the tumor microenvironment. Compared with antibody-directed enzyme prodrug therapy, gene-directed

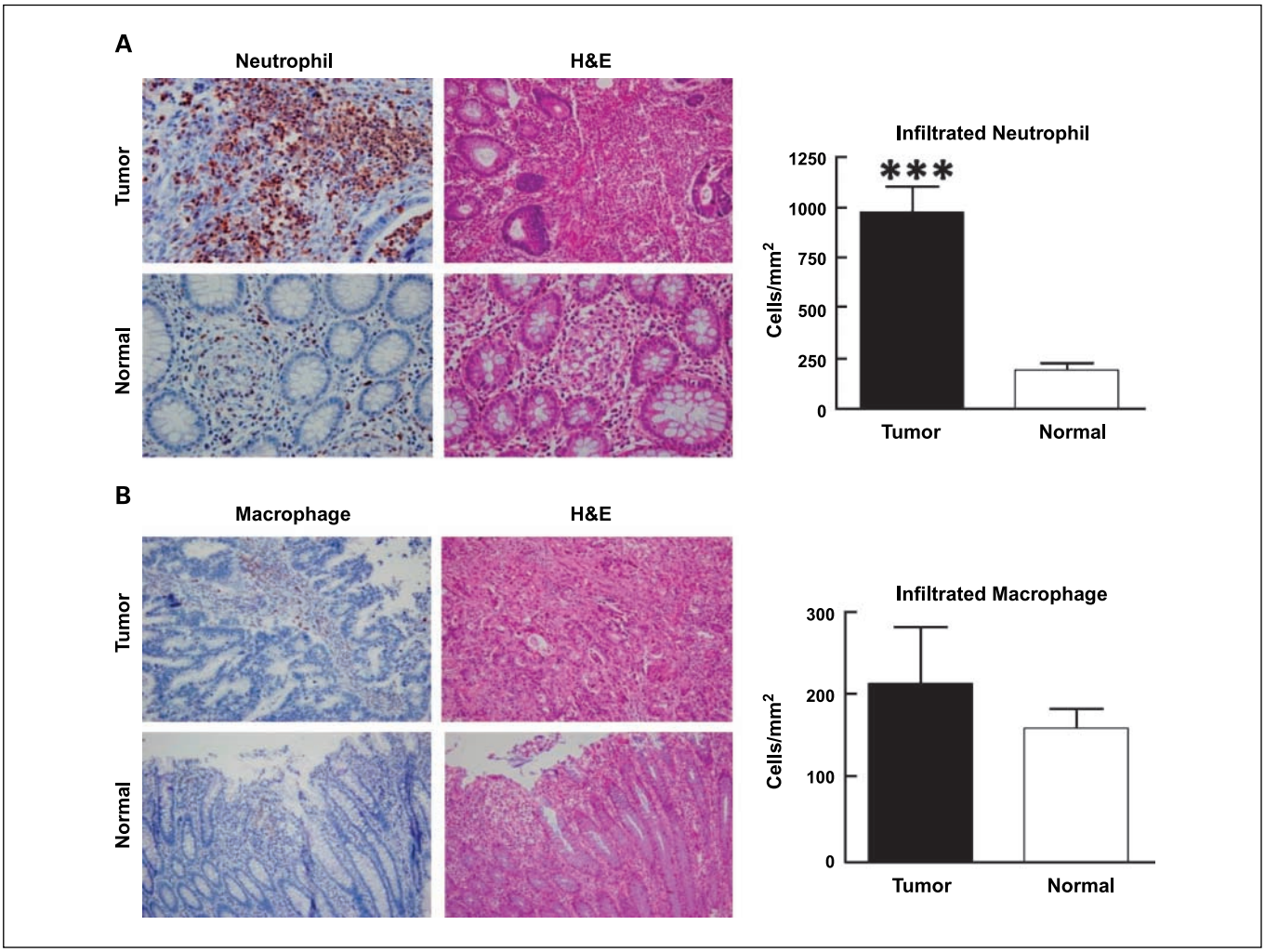

Fig. 6. Increased neutrophils and macrophages infiltration in human colon cancer. *A* and *B,* colon cancer specimens from 16 patients showed significantly infiltrated neutrophils and macrophages with positive Gr-1 and CD68 staining, respectively, compared with normal counterparts. The quantitative analysis showed a significant 10-fold increase of neutrophils in colon cancer tissues (n = 16) compared with their normal counterparts (n = 16). Macrophage infiltration was also increased in tumor tissues compared with normal counterparts. Bars, SE.

enzyme prodrug therapy, and virus-directed enzyme prodrug therapy, antiangiogenesis treatment is a much easier approach to effectively activate glucuronide prodrugs in the tumor microenvironment and achieve synergistic tumor inhibition effects for those resistant tumors with insufficient βG enzyme activity.

There are two possible mechanisms involved in DC101-mediated innate immune activation. First, DC101 directly induces endothelial cell apoptosis, which may release cytokines or chemokines that attract innate immune cell infiltration as commonly occurs in the inflammation process. Alternatively, DC101 may directly or indirectly induce cancer cell apoptosis, which further aggravates the inflammatory process and attracts more innate immune cells infiltration in the tumor microenvironment. Further studies are now under way to explore the mechanism of DC101-mediated innate immune activation in the tumor microenvironment.

Our prodrug delivery model also showed that DC101 promotion of prodrug delivery into tumors may be mediated by normalization of tumor vasculatures. The endothelial cells underwent apoptosis after treatment with DC101. These data are consistent with previous work showing that the underlying mechanisms involved in antiangiogenesis-mediated normalization of tumor vasculatures could attribute to pruning the immature vessels and fortifying the remaining ones (41, 49). The tumor vasculature under DC101 treatment becomes less tortuous, and the vessels are more uniformly covered by pericytes and basement membrane. Most importantly, normalization of tumor vasculature results in a decrease of vascular permeability and induces transvascular gradients in oncotic and hydrostatic pressure in tumors. The induced hydrostatic pressure gradient improves the penetration of prodrugs into tumors.

DC101 enhances inflammatory cell infiltration and normalizes tumor vasculatures, which provide a perfect tumor microenvironment for the 9ACG prodrug activation. Therefore, one single dose of 9ACG induced profound tumor cell apoptosis and tissue necrosis after DC101 treatment in prodrug-resistant colon tumors, which resulted in long-term tumor suppression and mice survival. The significant accumulation of neutrophils and macrophages in late-stage tumors

treated with 9ACG and DC101 suggested that innate immunity may be involved in the long-term suppression of resistant tumor growth. Interestingly, the number of natural killer cells showed no difference in PBS-treated or combined-treated tumors. In addition, fibrosis was significantly abundant in tumors treated with combined therapy, which suggested that combined therapy induced immune-mediated tissue damage. A single dose of 9ACG after DC101 treatment may induce a drastic necrotic tumor microenvironment, which further facilitates attraction of innate immune cell infiltration for inflammation-fibrosis cycling to eliminate tumor cells and induce fibrosis in late therapeutic stages. This interesting observation may provide an opportunity to design antiangiogenesis treatments followed by pulse therapy with high-dosage nontoxic prodrug administration for clinical trials instead of continuous therapy.

Our observations suggest that a combined treatment with agents altering the tumor microenvironment to promote continual infiltration of immune cells in the tumor environment, which is required to activate specific cytotoxic prodrugs, might be a potential strategy to develop novel targeting cancer therapies. The neutrophil infiltration in colorectal cancer tissues was highly statistically significant and 10-fold higher than their normal counterparts. These results clearly showed that innate immune cells were highly infiltrated in human colorectal cancer tissues and that they could serve as perfect targets for clinical trials by using monotherapy with the 9ACG prodrug in the near future. In particular, antiangiogenic factors may create optimal prodrug uptake pathways by normalizing tumor vessels for the 9AGC prodrug delivery and for activation by extracellular βG derived from increasing inflammatory cell infiltration in the tumor microenvironment. Our study provides *in vivo* evidence that the 9ACG prodrug has potential as a prodrug monotherapy or in combination with antiangiogenesis regimens in the treatment of cancer for clinical translation.

Disclosure of Potential Conflicts of Interest

No potential conflicts of interest were disclosed.

References

1. Dunn GP, Old LJ, Schreiber RD. The immunobiology of cancer immunosurveillance and immunoediting. Immunity 2004;21:137–48.
2. Balkwill F, Charles KA, Mantovani A. Smoldering and polarized inflammation in the initiation and promotion of malignant disease. Cancer Cell 2005;7:211–7.
3. Colombo MP, Mantovani A. Targeting myelomonocytic cells to revert inflammation-dependent cancer promotion. Cancer Res 2005;65:9113–6.
4. Pollard JW. Tumour-educated macrophages promote tumour progression and metastasis. Nat Rev Cancer 2004;4:71–8.
5. Bellocq A, Antoine M, Flahault A, et al. Neutrophil alveolitis in bronchioloalveolar carcinoma: induction by tumor-derived interleukin-8 and relation to clinical outcome. Am J Pathol 1998;152:83–92.
6. Bingle L, Brown NJ, Lewis CE. The role of tumour-associated macrophages in tumour progression: implications for new anticancer therapies. J Pathol 2002;196:254–65.
7. Condeelis J, Pollard JW. Macrophages: obligate partners for tumor cell migration, invasion, and metastasis. Cell 2006;124:263–6.
8. Giraudo E, Inoue M, Hanahan D. An aminobisphosphonate targets MMP-9-expressing macrophages and angiogenesis to impair cervical carcinogenesis. J Clin Invest 2004;114:623–33.
9. Huang S, Van Arsdall M, Tedjarati S, et al. Contributions of stromal metalloproteinase-9 to angiogenesis and growth of human ovarian carcinoma in mice. J Natl Cancer Inst 2002;94:1134–42.
10. Dirkx AE, Oude Egbrink MG, Wagstaff J, Griffioen AW. Monocyte/macrophage infiltration in tumors: modulators of angiogenesis. J Leukoc Biol 2006;80:1183–96.
11. Benelli R, Morini M, Carrozzino F, et al. Neutrophils as a key cellular target for angiostatin: implications for regulation of angiogenesis and inflammation. FASEB J 2002;16:267–9.
12. Scapini P, Morini M, Tecchio C, et al. CXCL1/macrophage inflammatory protein-2-induced angiogenesis *in vivo* is mediated by neutrophil-derived vascular endothelial growth factor-A. J Immunol 2004;172:5034–40.
13. Albini A, Sporn MB. The tumour microenvironment as a target for chemoprevention. Nat Rev Cancer 2007;7:139–47.
14. Rofstad EK, Mathiesen B, Kindem K, Galappathi K. Acidic extracellular pH promotes experimental metastasis of human melanoma cells in athymic nude mice. Cancer Res 2006;66:6699–707.
15. Ashby BS. pH studies in human malignant tumours. Lancet 1966;2:312–5.
16. Paigen K. Mammalian β-glucuronidase: genetics, molecular biology, and cell biology. Prog Nucleic Acid Res Mol Biol 1989;37:155–205.
17. Griffiths JR. Are cancer cells acidic? Br J Cancer 1991;64:425–7.
18. Stubbs M, McSheehy PM, Griffiths JR, Bashford CL. Causes and consequences of tumour acidity and implications for treatment. Mol Med Today 2000;6:15–9.
19. Netti PA, Hamberg LM, Babich JW, et al. Enhancement of fluid filtration across tumor vessels: implication for delivery of macromolecules. Proc Natl Acad Sci U S A 1999;96:3137–42.
20. Milosevic MF, Fyles AW, Hill RP. The relationship between elevated interstitial fluid pressure and blood flow in tumors: a bioengineering analysis. Int J Radiat Oncol Biol Phys 1999;43:1111–23.
21. Sevick EM, Jain RK. Measurement of capillary filtration coefficient in a solid tumor. Cancer Res 1991;51:1352–5.
22. Ferrara N, Alitalo K. Clinical applications of angiogenic growth factors and their inhibitors. Nat Med 1999;5:1359–64.
23. Jain RK. Molecular regulation of vessel maturation. Nat Med 2003;9:685–93.
24. Hellmann K. Recognition of tumor blood vessel normalization as a new antiangiogenic concept. Nat Med 2004;10:329; author reply -30.
25. Jain RK. Normalization of tumor vasculature: an emerging concept in antiangiogenic therapy. Science 2005;307:58–62.
26. Jain RK, Tong RT, Munn LL. Effect of vascular normalization by antiangiogenic therapy on interstitial hypertension, peritumor edema, and lymphatic metastasis: insights from a mathematical model. Cancer Res 2007;67:2729–35.
27. Willett CG, Boucher Y, di Tomaso E, et al. Direct evidence that the VEGF-specific antibody bevacizumab has antivascular effects in human rectal cancer. Nat Med 2004;10:145–7.
28. Batchelor TT, Sorensen AG, di Tomaso E, et al. AZD2171, a pan-VEGF receptor tyrosine kinase inhibitor, normalizes tumor vasculature and alleviates edema in glioblastoma patients. Cancer Cell 2007;11:83–95.
29. Lutz F, Igarashi T, Kinoshita T, et al. Mechanistic insights in the reversal of enantioselectivity of chiral catalysts by achiral catalysts in asymmetric autocatalysis. J Am Chem Soc 2008;130:2956–8.
30. Wani MC, Nicholas AW, Wall ME. Plant antitumor agents. 28. Resolution of a key tricyclic synthon, 5′(RS)-1,5-dioxo-5′-ethyl-5′-hydroxy-2′H,5′H,6′H-6′-oxopyrano[3′,4′- f]Δ 6,8-tetrahydro-indolizine: total synthesis and antitumor activity of 20(S)- and 20(R)-camptothecin. J Med Chem 1987;30:2317–9.
31. Wani MC, Nicholas AW, Manikumar G, Wall ME. Plant antitumor agents. 25. Total synthesis and antileukemic activity of ring A substituted camptothecin analogues. Structure-activity correlations. J Med Chem 1987;30:1774–9.
32. Li ML, Horn L, Firby PS, Moore MJ. Pharmacological determinants of 9-aminocamptothecin cytotoxicity. Clin Cancer Res 2001;7:168–74.
33. Giovanella BC, Hinz HR, Kozielski AJ, Stehlin JS, Jr., Silber R, Potmesil M. Complete growth inhibition of human cancer xenografts in nude mice by treatment with 20-(S)-camptothecin. Cancer Res 1991;51:3052–5.
34. Rubin E, Wood V, Bharti A, et al. A phase I and pharmacokinetic study of a new camptothecin derivative, 9-aminocamptothecin. Clin Cancer Res 1995;1:269–76.
35. Loos WJ, Verweij J, Gelderblom HJ, et al. Role of erythrocytes and serum proteins in the kinetic profile of total 9-amino-20(S)-camptothecin in humans. Anticancer Drugs 1999;10:705–10.
36. Prijovich ZM, Chen BM, Leu YL, Chern JW, Roffler SR. Anti-tumour activity and toxicity of the new prodrug 9-aminocamptothecin glucuronide (9ACG) in mice. Br J Cancer 2002;86:1634–8.
37. Prijovich ZM, Leu YL, Roffler SR. Effect of pH and human serum albumin on the cytotoxicity of a glucuronide prodrug of 9-aminocamptothecin. Cancer Chemother Pharmacol 2007;60:7–17.
38. Wolfe JH, Kyle JW, Sands MS, Sly WS, Markowitz DG, Parente MK. High level expression and export of β-glucuronidase from murine mucopolysaccharidosis VII cells corrected by a double-copy retrovirus vector. Gene Ther 1995;2:70.
39. Cheng TL, Chou WC, Chen BM, Chern JW, Roffler

SR. Characterization of an antineoplastic glucuronide prodrug. Biochem Pharmacol 1999;58:325–8.

40. Harada M, Imai J, Okuno S, Suzuki T. Macrophage-mediated activation of camptothecin analogue T-2513-carboxymethyl dextran conjugate (T-0128): possible cellular mechanism for antitumor activity. J Control Release 2000;69:389–97.

41. Tong RT, Boucher Y, Kozin SV, Winkler F, Hicklin DJ, Jain RK. Vascular normalization by vascular endothelial growth factor receptor 2 blockade induces a pressure gradient across the vasculature and improves drug penetration in tumors. Cancer Res 2004;64:3731–6.

42. Mantovani A, Allavena P, Sica A, Balkwill F. Cancer-related inflammation. Nature 2008;454:436–44.

43. Rooseboom M, Commandeur JN, Vermeulen NP. Enzyme-catalyzed activation of anticancer prodrugs. Pharmacol Rev 2004;56:53–102.

44. Huang PS, Oliff A. Drug-targeting strategies in cancer therapy. Curr Opin Genet Dev 2001;11:104–10.

45. Senter PD. Activation of prodrugs by antibody-enzyme conjugates: a new approach to cancer therapy. Faseb J 1990;4:188–93.

46. Leu YL, Roffler SR, Chern JW. Design and synthesis of water-soluble glucuronide derivatives of camptothecin for cancer prodrug monotherapy and antibody-directed enzyme prodrug therapy (ADEPT). J Med Chem 1999;42:3623–8.

47. Dubowchik GM, Walker MA. Receptor-mediated and enzyme-dependent targeting of cytotoxic anticancer drugs. Pharmacol Ther 1999;83:67–123.

48. Locigno R, Antoine N, Bours V, Daukandt M, Heinen E, Castronovo V. TNP-470, a potent angiogenesis inhibitor, amplifies human T lymphocyte activation through an induction of nuclear factor-κB, nuclear factor-AT, activation protein-1 transcription factors. Lab Invest 2000;80:13–21.

49. Manning EA, Ullman JG, Leatherman JM, et al. A vascular endothelial growth factor receptor-2 inhibitor enhances antitumor immunity through an immune-based mechanism. Clin Cancer Res 2007;13:3951–9.